Analysis of Triboelectric Charging of Particles due to Aerodynamic Dispersion by a Pulse of Pressurised Air Jet

M. Ali and M. Ghadiri*

School of Chemical and Process Engineering, University of Leeds, Leeds LS2 9JT, UK

*Email: m.ghadiri@leeds.ac.uk

ABSTRACT

Triboelectric charging of powders causes nuisance and electrostatic discharge hazards. It is highly desirable to develop a simple method for assessing the triboelectric charging tendency of powders using a very small quantity. We explore the use of aerodynamic dispersion by a pulse of pressurised air using the disperser of Morphologi G3 as a novel application. In this device particles are dispersed by injection of a pulse of pressurised air, the dispersed particles are then analysed for size and shape analysis. The high transient air velocity inside the disperser causes collisions of sample particles with the walls, resulting in dispersion, but at the same time it could cause triboelectric charging of the particles. In this study, we analyse this process by evaluating the influence of the transient turbulent pulsed-air flow on particle impact on the walls and the resulting charge transfer. Computational Fluid Dynamics is used to calculate particle trajectory and impact velocity as a function of the inlet air pressure and particle size. Particle tracking is done using the Lagrangian approach and transient conditions. The charge transfer to particles is predicted as a function of impact velocity and number of collisions based on a charge transfer model established previously for several model particle materials. Particles experience around ten collisions at different velocities as they are dispersed and thereby acquire charges, the value of which approaches the equilibrium charge level. The number of collisions is found to be rather insensitive to particle size and pressure pulse, except for fine particles, smaller than about 30 µm. As the particle size is increased, the impact velocity decreases, but the average charge transfer per particle increases, both very rapidly. Aerodynamic dispersion by a gas pressure pulse provides an easy and quick assessment of triboelectric charging tendency of powders.

INTRODUCTION

During powder transport, particles collide with the containing walls and with each other, resulting in triboelectric charging (Bailey, 1984). Triboelectric charging in powder processing is generally undesirable as it results in reduced powder flowability and can also pose safety issues such as dust explosion. The current state of understanding has been reviewed by Matsusaka et al. (2010). Organic powders such as active pharmaceutical ingredients and excipients are particularly prone to extensive charging (Supuk et al., 2012). In pharmaceutical industry this can lead to uneven dosage of APIs in formulations. It is therefore important to understand and control the charging behaviour of particles during powder handling.

The charge transfer to/from a single particle impacting a wall has been investigated by various researchers including Masui and Murata (1983; 1984), Yamamoto and Scarlett (1986), Matsuyama and Yamamoto (1989; 1994; 1995 a-c; 1997; 2006), Matsusaka et al. (2003 & 2007), Matsuyama et al. (2003 & 2009), Ema et al. (2003) and recently reviewed by Matsusaka et al. (2010). The charge transfer in a single impact depends on the initial charge on the particle, the impacting particle velocity which in turn affects the contact area. Based on the work of Matsusaka et al. (2000), charge transfer in an impact process takes place during the unloading stage and its magnitude is linearly proportional to the maximum deformed contact area. Matsuyama and Yamamoto (1995c) found that the charge transfer on impact is dependent on the particle initial charge and there is a limiting value beyond which the particle no longer gains further charges, referred to as the equilibrium charge. Zarrebini et al. (2013) used the disperser of Morphologi G3 (Malvern Instruments, Worcestershire, UK) to measure the triboelectric charging of powders and found it to be an efficient way to evaluate the triboelectric charging of bulk solids, requiring only a small sample quantity. The design of this disperser has changed from the metal foil rupture as evaluated by Zarrebini et al. (2013) to the one shown in Figure 1. The capsule comprises two parts, a bottom part having a sample well, where a small quantity of powder is placed and a top part for dispersion. The two parts are dovetailed and sealed via an O-ring. A pulse of pressurised air is injected from the top, causing rapid dispersion by collisions of powder particles with surrounding walls within the capsule. The dispersed powder comes out from the bottom outlets of the capsule.

Recently, Alfano (2016) used this disperser to characterise the triboelectric charging of pharmaceutical powders. The transferred charge per unit mass (referred to as charge to mass ratio) acquired by the particles was found to be inversely proportional to the diameter of the particles. An inverse relationship was also found between the charge to mass ratio and the volume of sample.

In this study, numerical modelling is carried out to predict the trajectory of the particles, their impact velocities and the corresponding charging behaviour using the new Morphologi G3 disperser. The air flow inside the disperser is turbulent and transient, hence to capture the effect of turbulence on the predicted particles trajectories and impact velocities, Computational Fluid Dynamics (CFD) modelling approach is used.

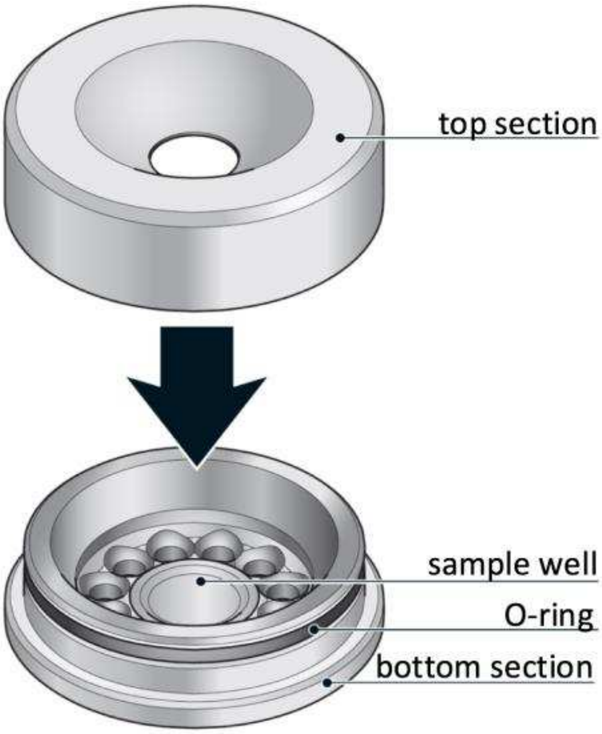

Figure – 1: Morphologi G3 dispersion capsule (courtesy of Malvern Instruments)

CFD MODELLING

CONTINUOUS PHASE

The continuous phase is air and its flow is modelled using the continuity and Navier-Stokes equations (Versteeg and Malalasekera, 1995) with three-dimensional, transient flow assumption. The turbulence is modelled using the scale adaptive simulation model (Menter and Egorov, 2010) due to its advantage in better prediction of fluid velocity profiles in flows of transient nature. The method gives a better prediction of turbulence compared to the eddy viscosity based and Reynolds Stress turbulence models (Egorov et al. (2010)). The modelling of flow near the wall is carried out using standard wall functions with smooth wall assumption. The air is considered to be compressible as the density of the air is expected to vary significantly due to large variations in pressure particularly at higher inlet pressures.

DISCRETE PHASE

The discrete phase comprises spherical particles which are initially placed in the sample well. The particles get dispersed due to a pulse of pressurised air injected from the top. The coupling between the air and particles is one-way, i.e. the air flow influences the trajectories of the particles, but the momentum exerted by the particles on the gas phase is ignored. This assumption is valid for particulate flows which are very lean. The particle trajectory is computed by solving the equation of motion of particles considering the drag, gravitational and buoyancy forces. A widely used spherical drag law proposed by Morsi and Alexander (1972) is used for the calculation of drag coefficient. The dispersion of particles due to turbulence is taken into account by enabling the discrete random walk model (Ansys, 2016). The impact of particles on the walls causes the particles to acquire charges. The charge build-up on the particles is taken into account considering only particle-wall collisions. The charge transfer between particles due to inter-particle collisions is ignored. The space charge effect is also neglected. Similarly, any possible breakage of particles due to high-velocity wall impact is also not considered. The restitution coefficient (defined as the ratio between the rebound and incident velocities) is assumed to be 0.5 for both normal and tangential components for all the particle sizes considered. Charge transfer upon impact is given by:

$$\frac{\Delta q}{\alpha \Delta s} + \frac{q_i}{q_{max}} = 1 \qquad (1)$$

where Δq is the amount of charge transferred to the particle, q_i is the impacting particle charge, q_{max} is the equilibrium charge and Δs is the maximum contact area due to elastic-plastic impact between a particle and a plane, calculated using the equation proposed by Masuda et al. (1976):

$$\Delta s = 0.41 p D_p^2 \rho^{1/2} Y^{-1/2} (V_{in} - V_y) \qquad (2)$$

where D_p is particle diameter, ρ is particle density, Y is yield stress and V_{in} and V_y are normal impact velocity and impact velocity at which yielding occurs, respectively.

Computational Details, Numerical Solution Method and Initialisation

The meshing of the disperser was carried out using Ansys Meshing (Ansys, 2016). A sensitivity analysis was carried out to ensure that the results are mesh independent. The selected mesh comprised 8.0×10^5 primarily tetrahedral cells and is depicted in Figure 2. The conservation equations for the continuous and discrete phases are solved using the commercial CFD software Fluent v. 16 (Ansys, 2016) for compressible flows. For the inlet boundary condition, the pressure is specified at the inlet face with values varying for different cases. The outlet pressure with a value of 0 barg is specified at the outlet face. For the turbulence boundary conditions, a turbulence intensity of 5% at the corresponding faces along with its hydraulic diameter is specified.

The pressure-velocity coupling is carried out using the SIMPLE scheme. The convective terms are discretised using the second-order upwind discretisation scheme. The time step for tracking of the particles and the continuous phase was set to 5.0×10^{-6} s. The simulation was allowed to run at the specified inlet air pressure up to 0.02 s, to allow the pulse of air to enter the dispersion capsule and disperse the particles. Thereafter, the inlet pressure was changed to 0 barg pressure and the simulation was continued until all the particles exit from the bottom. The impact charge on each particle was calculated using the impacting particle velocity upon each particle-wall contact using equations (1) and (2) which were incorporated using user-defined functions (UDF) in Fluent.

To assess the influence of increasing inlet air pressure on the charge acquired by the particles, the inlet air pressure was varied in the range of 0.5 to 3 barg. Spherical particles having characteristics of aspirin and α-lactose monohydrate (α-LM), i.e. equilibrium charges of -40 pC and -18 pC, respectively, (as previously measured by Watanabe et al., 2006) were used in the case studies. Different particle sizes were considered as the particle trajectory is dependent upon its size. The particle sizes investigated in this study are: 10, 20, 30, 50, 75, 100, 150 and 200 µm diameter particles. The density of both aspirin and α-LM is taken as 1500 kg/m^3.

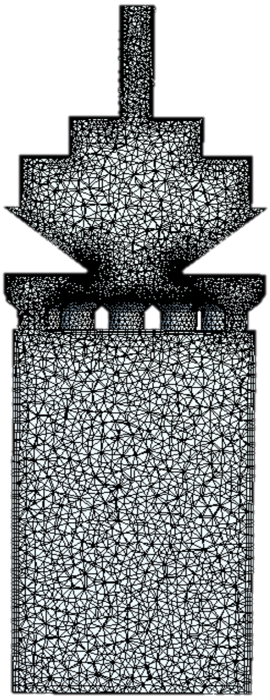

Figure – 2: Cross-sectional view of the mesh used for CFD analysis

MODELLING RESULTS AND DISCUSSION

Figure 3 is a plot of cross-sectional view of the disperser with contours coloured by air velocity magnitude after a pulse of air is introduced into the disperser (taken at 0.02 s), at different inlet air pressures. A high velocity jet of air is observed as it exits the inlet nozzle. The jet impinges on the sample well dispersing the powder sample. It can be observed that the air jet maximum velocity becomes supersonic at pressures above 1 barg.

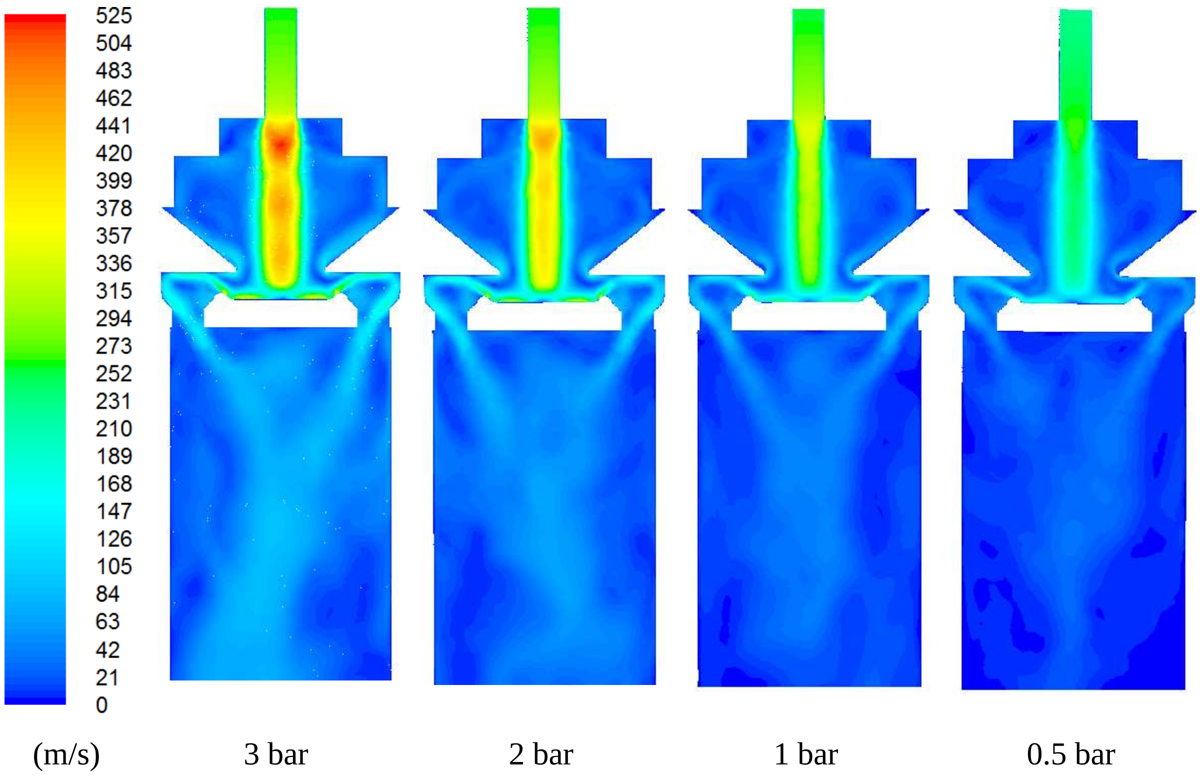

Figure – 3: Contours of air velocity magnitude at different inlet air pressures

Figure 4a is a plot of selected trajectories of 10 μm and 50 μm particles coloured by their velocity magnitude for an inlet air pressure of 1 barg. The particles acquire the highest velocity in the sample well region, thereafter, the velocity decreases. All the particles collide with the wall above the sample well and after a number of collisions they exit from the nozzles below the capsule. Hence the particles are expected to acquire more charge near the sample well region. The impact velocity of 10 μm particles is larger than that of the 50 μm particles, as the smaller particles have less inertia and get accelerated by the air flow much faster. A typical example of the particle impact velocity as a function of the collision number as the particle is dispersed is shown in Figure 4b. In this case 15 collisions have occurred at different velocities. Different particles experience different number of collisions and impact velocities, so for each particle size 1000 trajectories were calculated.

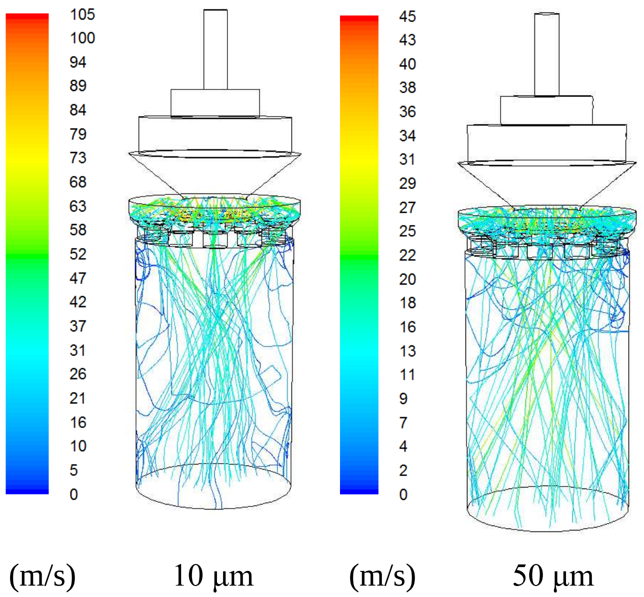

Figure – 4a: Trajectories of particles inside the disperser coloured by particle velocity magnitude

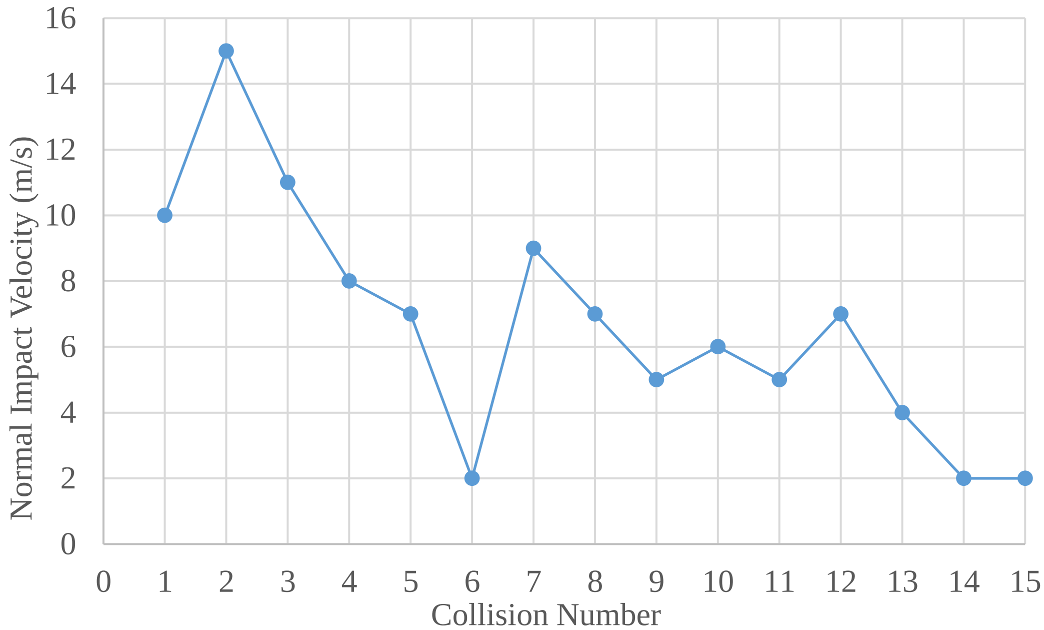

Figure – 4b: Normal impact velocity of a 200 µm aspirin particle at 2 barg pressure

Figure 5 is a plot of impact charge acquired by four trajectories, shown in different colours, of 200 µm spherical particles with aspirin properties as a function of collision number at 2 barg inlet pressure. Each particle behaves differently due to turbulence in the air flow, resulting in different number of collisions inside the disperser. The charge acquired by the particles increases with each collision.

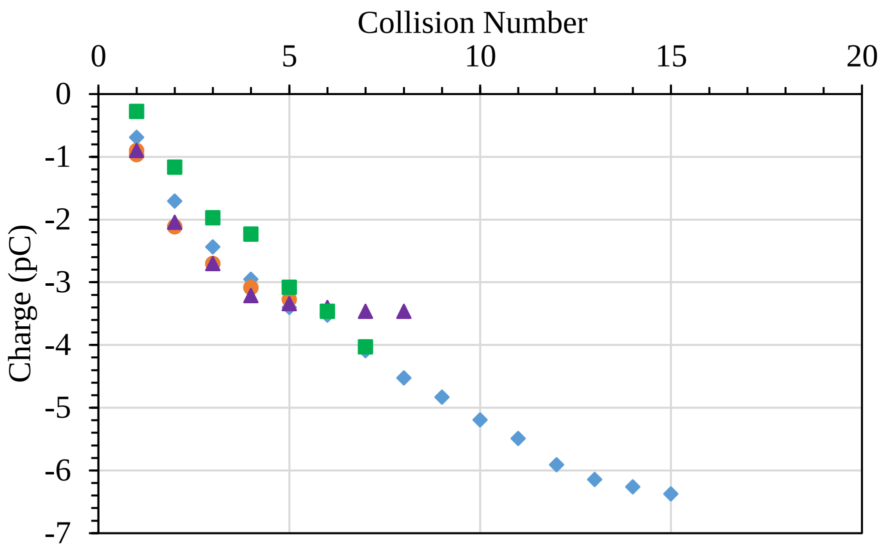

Figure – 5: Impact charge acquired by four 200 μm spherical particles representing aspirin as a function of collision number; legends showing different particles.

Figure 6 is a plot of the average number of collisions experienced by aspirin particles of different sizes before exiting the disperser at different inlet air pressures. For each size and pressure, 1000 trajectories were simulated. It can be observed that the average number of collisions experienced by the particles is relatively insensitive to the inlet air pressure used in the Morphologi G3 disperser except particles smaller than 30 μm, for which the average number of collisions in general increases with increasing inlet air pressure.

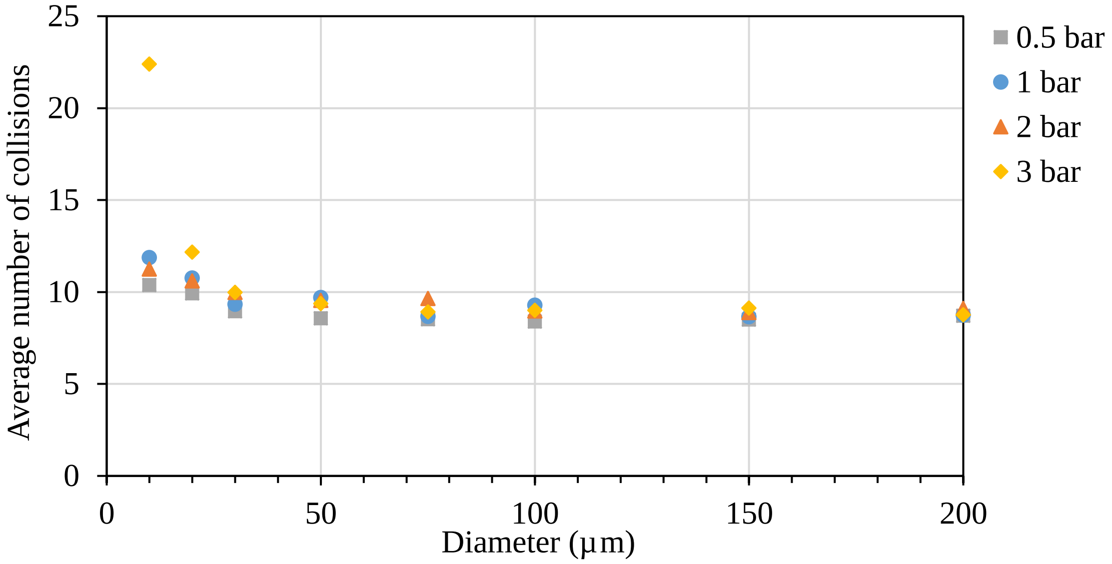

Figure – 6: Average number of collisions within the disperser as a function of particle size

Figure 7 is a plot of the average maximum impact velocity of spheres with aspirin particle properties of different sizes obtained using different inlet air pressures. The maximum impact velocity decreases initially very rapidly with size for each inlet air pressure, but then very slowly for particles greater than about 70 µm. The maximum impact velocity is the highest for the highest inlet air pressure as expected since the jet velocity is greater at higher pressures (Figure 3).

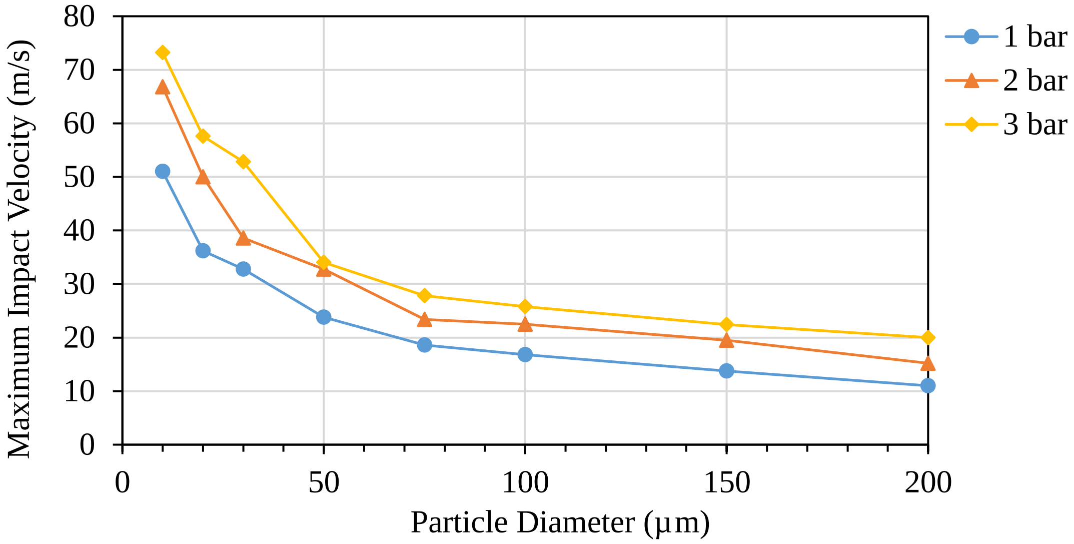

Figure – 7: Average maximum impact velocity within the disperser for different particle sizes

Figure 8 is a plot of the average charge acquired by spherical particles with aspirin properties of different sizes exiting the disperser for different inlet air pressures. Smaller particles acquire lower charge compared to larger particles. The charge acquired by the particles increases almost exponentially with size, even though the maximum impact velocity decreases with size (Figure 7). Larger particles have greater contact area, hence resulting in larger charge accumulation. Inlet pressure of 3 barg pressure results in the highest charge accumulation compared to lower pressures.

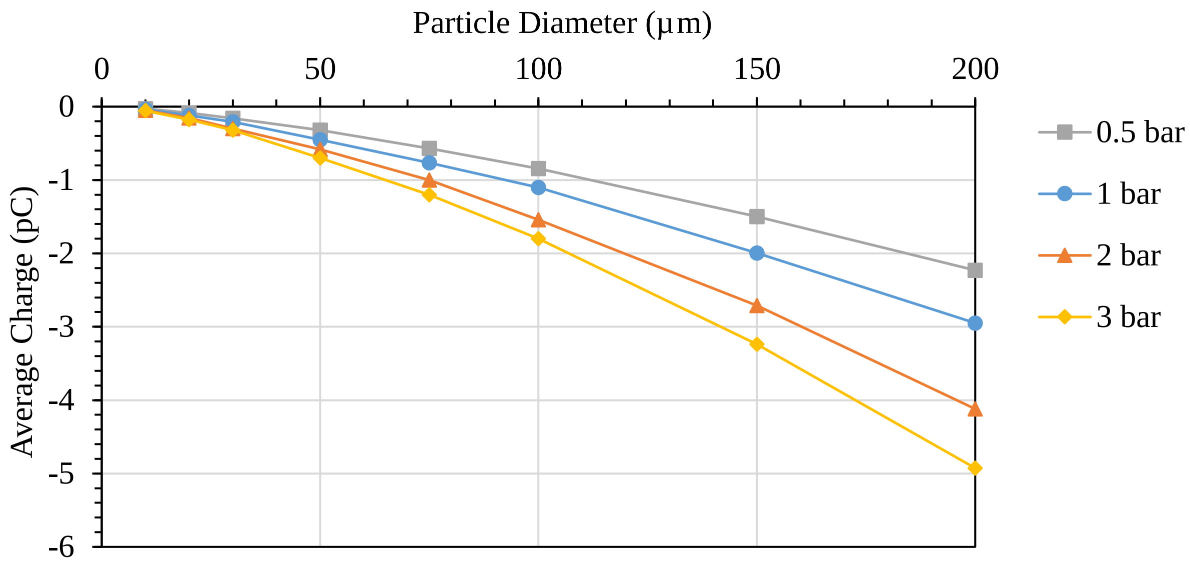

Figure – 8: Average charge acquired by aspirin particles exiting the disperser as a function of particle size

Figure 9 is a plot of the average charge acquired by α-LM particles exiting the disperser. The trend is similar to the plot obtained for aspirin particles, however, the average charge acquired by α-LM particles is lower.

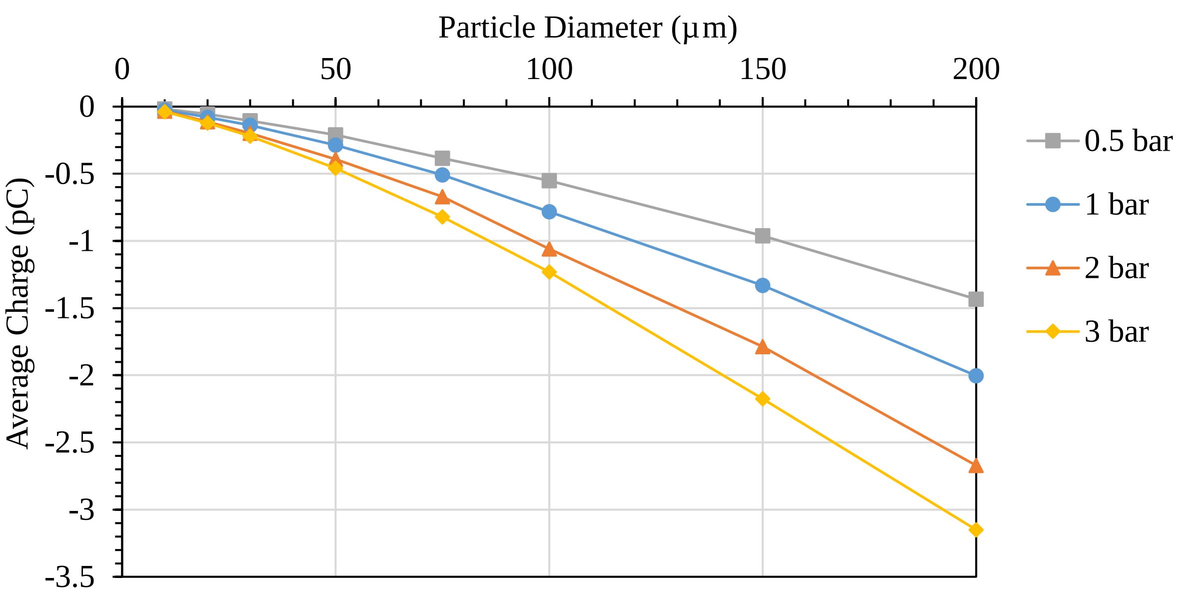

Figure – 9: Average charge acquired by α-LM particles exiting the disperser as a function of particle size

The predicted average charge to mass ratio is depicted in Figure 10 (a) and (b) for aspirin and α-LM, respectively. The charge to mass ratio decreases with increasing particle size, even though the total charge acquired by the larger particles is higher. Aspirin has a higher charge to mass ratio for a given pressure compared to α-LM and the ratio between the charge to mass ratios of aspirin and α-LM is ≈ 1.5.

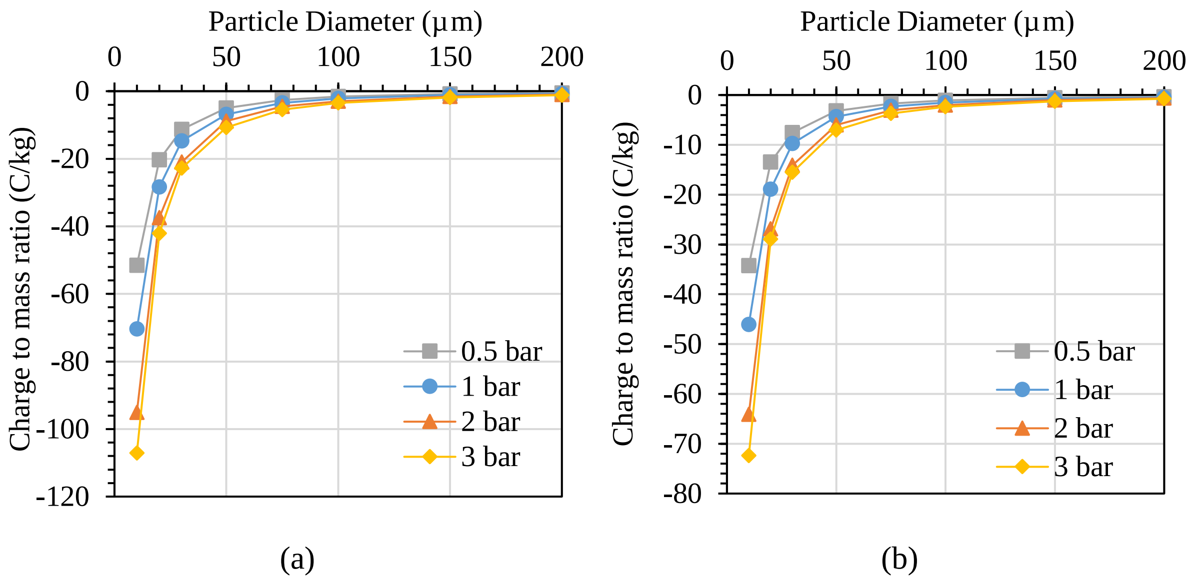

Figure – 10: Average charge to mass ratio acquired by the particles at different pressures: (a) Aspirin; (b): α-LM

Conclusions

Three-dimensional CFD modelling of Morphologi G3 disperser has been carried out to analyse the air flow dynamics, particle trajectories and charging behaviour of particles of different sizes at several inlet air pressures. The aerodynamics of a high air velocity jet impinging on a sample well, causing particle dispersion, has been analysed. It is found that particles smaller than 100 µm exhibit higher impact velocities and their number of collisions gets more affected by the inlet air pressure. The larger particles (>100 µm) are relatively insensitive to the inlet air pressure in terms of the number of collisions within the disperser. Although the larger particles have lower impact velocities compared to the smaller particles, they acquire more charges due to greater contact surface area. It is found that aspirin acquires 1.5 times more charge compared to α-lactose monohydrate. Aerodynamic dispersion by a gas pressure pulse provides an easy and quick assessment of triboelectric charging tendency of powders using a very small quantity.

Acknowledgement

The authors are grateful to Dr Paul Kippax, Malvern Instruments, for providing design information on the Morphologi G3 disperser.

REFERENCES

Alfano, F. O. (2016). Evaluation of a new dispersion technique for measuring triboelectric charging of particles. MSc. Dissertation, University of Leeds.

Ansys (2016). ANSYS® Academic Research, Release 16.2.

Bailey, A.G. (1984), Electrostatic phenomena during powder handling. Powder Technology, vol. 37, pp. 71-85.

Egorov, Y., Menter, F. R., Lechner, R. and Cokljat, D. (2010). The scale-adaptive simulation method for unsteady turbulent flow predictions. Part 2: Application to complex flows. Flow Turbulence Combust., v. 85, pp. 139-165.

Ema, A. Yasuda, D., Tanoue, K., Masuda, H. (2003). Tribo-charge and rebound characteristics of particles impact on inclined or rotating metal target. Powder Technology 135/136, 2-13.

Masuda, H., Komatsu, T. and Iinoya, K. (1976). AIChE J., vol. 22(3), pp. 558-564.

Masui, N. and Murata,Y. (1983). Electrification of polymer particles by impact on a metal plate. Japanese Journal of Applied Physics 22, pp. 1057–1062.

Masui, N. and Murata,Y. (1984). Mechanisms of charge build-up on a polymer particle by repeated impact. Japanese Journal of Applied Physics 23, pp. 550–555.

Matsusaka, S., Ghadiri, M. and Masuda, H. (2000). Electrification of an elastic sphere by repeated impacts on a metal plate. J. Phy. D: Appl. Phys., vol. 33, pp. 2311-2319.

Matsusaka, S., Nishida, T., Gotoh, Y., Masuda, H. (2003). Electrification of fine particles by impact on a polymer film target Advanced Powder Technology 14, 127-138.

Matsusaka, S., Oki, M., Masuda, H. (2007). Control of electrostatic charge on particles by impact charging. Advanced Powder Technology 18, 229-244.

Matsusaka, S., Maruyama, H., Matsuyama, T. and Ghadiri, M. (2010). Triboelectric charging of powders: A review. Chemical Engineering Science, vol. 65, pp. 5781-5807.

Matsuyama, T., Supuk, E., Ahmadian, H., Hassanpour, A. and Ghadiri, M. (2009). Analysis of tribo-electric charging of spherical beads using distinct element method. AIP Conference Proceedings, v. 1145 (1), DOI: 10.1063/1.3179845.

Matsuyama, T., Ogu, M., Yamamoto, H., Marijnissen, J.C.M. and Scarlett, B. (2003). Impact charging experiments with single particles of hundred micrometre size. Powder Technology 135/136, pp. 14–22.

Matsuyama, T. and Yamamoto, H. (1989). Charge transfer between a single polymer particle and a metal plate due to impact. KONA 7, pp. 15–21.

Matsuyama, T. and Yamamoto, H. (1994). Charge transfer between a polymer particle and a metal plate due to impact. IEEE Transactions on Industry Applications 30, pp. 602–607.

Matsuyama, T. and Yamamoto, H. (1995a). Charge relaxation process dominates contact charging of a particle in atmospheric conditions. Journal of Physics D: Applied Physics 28, pp. 2418–2423.

Matsuyama, T. and Yamamoto, H. (1995b). Electrification of single polymer particles by successive impacts with metal targets. IEEE Transactions on Industry Applications 31, pp. 1441–1445.

Matsuyama, T. and Yamamoto, H. (1995c). Characterizing the electrostatic charging of polymer particles by impact charging experiments. Advanced Powder Technology 6, pp. 211–220.

Matsuyama, T. and Yamamoto, H. (1997). Charge relaxation process dominates contact charging of a particle in atmospheric conditions II. General model. Journal of Physics D: Applied Physics 30, pp. 2170–2175.

Matsuyama, T. and Yamamoto, H. (2006). Impact charging of particulate materials, Chemical Engineering Science, vol. 61, pp. 2230-2238.

Menter, F. R. and Egorov, Y. (2010). The scale-adaptive simulation method for unsteady turbulent flow predictions. Part 1: Theory and model description. Flow Turbulence and Combustion, v. 85, pp. 113-138.

Morsi, S. A. and Alexander, A. J. (1972). An investigation of particle trajectories in two-phase flow systems. J. Fluid Mech., vol. 55 (2), pp. 193-208.

Supuk, E., Zarrebini, A., Reddy, J. P., Hughes, H., Leane, M. M., Tobyn, M. J., Timmins, P. and Ghadiri, M. (2012). Tribo-eletrification of active pharmaceutical ingredients and excipients. Powder Technology, vol. 217, pp. 427-434.

Versteeg, H. K. and Malalasekera, W. (1995). An Introduction to Computational Fluid Dynamics. Longman Scientific and Technical, Harlow.

Watanabe, H., Samimi, A., Ding, Y. L., Ghadiri, M., Matsuyama, T., Pitt, K. G. (2006). Measurement of charge transfer due to single particle impact. Part. Part. Syst. Charact., vol. 23, pp. 133-137.

Yamamoto, H. and Scarlett, B. (1986). Triboelectric charging of polymer particles by impact. Particle Characterization 3, pp. 117–121.

Zarrebini, A., Ghadiri, M., Dyson, M., Kippax, P. and McNeil-Watson, G. (2013). Tribo-electrification of powders due to dispersion. Powder Technology, vol. 250, pp. 75-83.